Essential Thiol Requirement To Restore Pterin- or Substrate-Binding Capability and To Regenerate Native Enzyme-Type High-Spin Heme Spectra in the *Escherichia coli*-Expressed Tetrahydrobiopterin-Free Oxygenase Domain of Neuronal Nitric Oxide Synthase[†]

Masanori Sono,*[,‡] Amy P. Ledbetter,[‡] Kirk McMillan,[§] Linda J. Roman,[||] Thomas M. Shea,[||] Bettie Sue Siler Masters,[||] and John H. Dawson*[,‡,⊥]

Department of Chemistry and Biochemistry and School of Medicine, University of South Carolina, Columbia, South Carolina 29208, Department of Biochemistry, The University of Texas Health Science Center, San Antonio, Texas 78284-7760, and Pharmacopeia, Inc., Cranbury, New Jersey 08512

Received July 8, 1999; Revised Manuscript Received September 24, 1999

ABSTRACT: Nitric oxide (NO) synthases (NOS) are thiolate-ligated heme-, tetrahydrobiopterin (BH_4)-, and flavin-containing monooxygenases which catalyze the NADPH-dependent conversion of L-arginine (L-Arg) to NO and citrulline. NOS consists of two domians: an N-terminal oxygenase (heme- and BH_4-bound) domain and a C-terminal reductase (FMN- and FAD-bound) domain. In this study, we have spectroscopically examined the binding of L-Arg and BH_4 to the dimeric, BH_4-free ferric neuronal NOS (nNOS) oxygenase domain expressed in *Escherichia coli* separately from the reductase domain. Addition of L-Arg or its analogue inhibitors (N^G-methyl-L-Arg, N^G-nitro-L-Arg) and BH_4, together with dithiothreitol (DTT), to the pterin-free ferric low-spin oxygenase domain (λ_{max}: 419, 538, 568 nm) and incubation for 2−3 days at 4 °C converted the domain to a native enzyme-type, predominantly high-spin state (λ_{max}: ∼395, ∼512, ∼650 nm). 7,8-Dihydrobiopterin and other thiols (e.g., β-mercaptoethanol, cysteine, and glutathione, with less effectiveness) can replace BH_4 and DTT, respectively. The UV−visible absorption spectrum of L-Arg-bound ferric full-length nNOS, which exhibits a relatively intense band at ∼650 nm ($\epsilon = 7.5-8$ mM^{-1} cm^{-1}) due to the presence of a neutral flavin semiquinone, can then be quantitatively reconstructed by combining the spectra of equimolar amounts of the oxygenase and reductase domains. Of particular note, the heme spin-state conversion does not occur in the absence of a thiol even after prolonged (35−48 h) incubation of the oxygenase domain with BH_4 and/or L-Arg under anaerobic conditions. Thus, DTT (or other thiols) plays a significant role(s) beyond keeping BH_4 in its reduced form, in restoring the pterin- and/or substrate-binding capability of the *E. coli*-expressed, BH_4-free, dimeric nNOS oxygenase domain. Our results in combination with recently available X-ray crystallography and site-directed mutagenesis data suggest that the observed DTT effects arise from the involvement of an intersubunit disulfide bond or its rearrangement in the NOS dimer.

The inorganic free radical gas nitric oxide (NO)[1] functions as a neurotransmitter in the brain cerebellum and as a blood flow-controlling factor in endothelial cells. NO is also generated as a cytotoxic agent in macrophages. NO is synthesized in vivo from L-Arg and O_2 by a family of spectrally P450-like, but flavin (FMN and FAD)- and tetrahydrobiopterin (BH_4)-containing heme proteins called nitric oxide synthases (NOS) through NADPH-dependent monooxygenation reactions (for selected reviews, see refs *1*−*5*).

Three isoforms of NOS are known which have considerable amino acid sequence homology (50−60%) to each other, but differ in certain aspects. Brain neuronal (constitutive)

[†] This research was supported by National Institutes of Health Grants GM-26730 (to J.H.D.) and HL-30050 and GM-52419 (to B.S.S.M.), from the United States Public Health Service, and by Grant AQ-1192 from the Robert A. Welch Foundation (to B.S.S.M.). A portion of this paper will be submitted by A.P.L. in partial fulfillment of the Ph.D. requirements at the University of South Carolina.

* To whom correspondence should be addressed at the Department of Chemistry and Biochemistry, University of South Carolina, Columbia, SC 29208. Phone: 803-777-5726 (M.S.) or 803-777-7234 (J.H.D.). Fax: 803-777-9521. E-mail: msono@psc.sc.edu (M.S.) or dawson@psc.sc.edu (J.H.D.).

[‡] Department of Chemistry and Biochemistry, University of South Carolina.

[§] Pharmacopeia, Inc.

[||] The University of Texas Health Science Center at San Antonio.

[⊥] School of Medicine, University of South Carolina.

[1] Abbreviations: NO, nitric oxide; P450, cytochrome P450; BH_4, (6*R*)-5,6,7,8-tetrahydrobiopterin; BH_2, 7,8-dihydrobiopterin; 4-amino-BH_4, 2,4-diamino-5,6,7,8-tetrahydro-6-(L-*erythro*-1,2-dihydroxypropyl)-pteridine; NOS, nitric oxide synthase; "nNOS, iNOS, and eNOS", brain neuronal, macrophage (inducible), and endothelial nitric oxide synthases, respectively; CaM, calmodulin; $P450_{BM-3}$, fatty acid-hydroxylating cytochrome P450 isolated from *Bacillus megaterium*; P450-CAM, camphor-hydroxylating cytochrome P450 isolated from *Pseudomonas putida*; DTT, dithiothreitol; BME, β-mercaptoethanol; EDTA, ethylenediaminetetraacetic acid; Tris, tris(hydroxymethyl)aminomethane; NNA, N^G-nitro-L-Arginine; NMA, N^G-methyl-L-Arginine; MCD, magnetic circular dichroism.

10.1021/bi991580j CCC: $18.00
Published on Web 11/05/1999

NOS (nNOS) has ~220 N-terminal amino acid extra residues (containing the so-called "GLGF motif") that probably serve as an intracellular anchor domain for cellular protein−protein interactions, resulting in cellular localization of this isoform (*6*). Thus, nNOS (~160 kDa) is considerably larger than the endothelial (constitutive) (eNOS) and macrophage (inducible) (iNOS) (~130 kDa for the latter two) isoforms. Among the three isoforms, only eNOS is membrane-associated through myristoylation of its N-terminal residues; nNOS and iNOS are cytosolic.

NOS is only catalytically active in its homodimeric form (*7*−*9*). The C-terminal half of NOS consists of the reductase domain (~80 kDa) which contains the NADPH-binding site and protein-bound FAD and FMN. The latter two prosthetic groups serve as an electron-transport chain from NADPH to the N-terminal half, the oxygenase (heme-bound) domain (*1*−*5*). The two domains are connected by a calmodulin (CaM)-binding module. The binding of Ca^{2+}-CaM serves as a switch for interdomain electron transfer to initiate catalysis (*10*). Thus, NOS is a catalytically self-sufficient monooxygenase similar to $P450_{BM-3}$ from *Bacillus megaterium* (*11*) except that the latter does not require BH_4 and Ca^{2+}-CaM. The NOS reductase domain shares striking sequence homology with mammalian NADPH−P450 reductase, as well as with the reductase domain of $P450_{BM-3}$. In contrast, the oxygenase domain of nNOS has a sequence that distinctly differs from those of P450s, thereby excluding NOS from the cytochrome P450 gene family. Recent X-ray crystal structures of the BH_4- and L-Arg-bound dimeric iNOS and eNOS oxygenase domains (*12*−*15*) have, in fact, revealed structural distinctions between NOS and P450 as well.

Among the four NOS prosthetic groups, FAD, FMN, heme, and BH_4, the first three components serve as redox cofactors. The exact role(s) of BH_4 in NOS catalysis remain(s) to be clarified. Previous studies have indicated that BH_4 is required to stabilize the catalytically active dimeric structure of NOS (*16*, *17*). Yet, more recent studies have also implicated BH_4 in redox reactions in the NOS catalysis either as a two-electron-transferring cofactor (*18*, *19*) as in aromatic amino acid hydroxylases (*20*, *21*) or as a unique one-electron-transferring redox cofactor (*13*, *22*). Recently, the intact (full-length) as well as the separated oxygenase and reductase domains of the three recombinant NOS isoforms have been successfully expressed in *E. coli* (*8*, *23*−*26*). Since *E. coli* lacks the BH_4 synthesis system (*27*), this expression technique has enabled researchers to prepare completely BH_4-free NOS proteins. This has made it possible to study the effects of BH_4 on the spectral, structural, and catalytic properties of intact NOS, as well as its separated oxygenase domain.

The *E. coli*-expressed, BH_4- and substrate (L-Arg)-free oxygenase (heme-bound) domain of rat nNOS exhibits a largely low-spin-type electronic absorption spectrum (*23*), in sharp contrast to the predominantly high-spin-type spectral properties of BH_4-bound, Arg-free native full-length nNOS (*28*, *29*). In the present study, we have examined the binding of BH_4 as well as substrate or inhibitors to the pterin-free, dimeric nNOS oxygenase domain. We have been able to convert the low-spin oxygenase domain to a native enzyme-type high-spin form by addition of L-Arg and BH_4 together with DTT. The characteristic electronic absorption spectrum of full-length ferric nNOS containing bound BH_4 and L-Arg, which is somewhat unusual because of the presence of a neutral semiquinone as compared with the spectra of other thiolate-ligated heme-containing proteins (*29*), has then been successfully reconstructed from both the oxygenase and reductase domains.[2] Interestingly, however, we have observed that the heme spin-state conversion, i.e., BH_4 and/or L-Arg binding to the domain, does not occur without a thiol even under anaerobic conditions where BH_4 is kept in its fully reduced form. The significance of this finding is discussed in relation to an intersubunit disulfide bond (*12*, *15*) or intersubunit $Zn(Cys)_4$ metal center (*13*−*15*) which has been recently revealed by X-ray crystallography for the dimeric iNOS and eNOS oxygenase domains.

EXPERIMENTAL PROCEDURES

Materials. BH_4, 4-amino-BH_4, and BH_2 were purchased from Research Biochemicals, BIOMOL Research Laboratories, and Dr. B. Schirck's laboratory (Jona, Switzerland), respectively. N^G-Nitro-L-Arg (NNA) and N^G-methyl-L-Arg (NMA) were purchased from Alexis Biochemicals. CO and argon gases were obtained from Matheson Co. All other chemicals including L-Arg and L-thiocitrulline were purchased from Sigma or Aldrich and used as received.

Preparation of Full-Length nNOS and the Separated nNOS Oxygenase (Heme-Bound) and Reductase (Flavin-Bound) Domains. E. coli-expressed full-length rat brain nNOS and its separately expressed, heme-containing oxygenase domain (the N-terminal 714 amino acid residues) and the flavin-containing reductase domain (amino acid residues 715−1429) were prepared as described previously (*23*, *24*). Concentrated full-length nNOS protein and the oxygenase domain (~100 μM on the basis of heme) were stored at −70 °C in 50 mM Tris-HCl (pH 7.4) containing 10% glycerol, 1 mM BME, and 150 mM NaCl. The stock solutions of the reductase domain (~120 μM) were also stored in the same buffer without BME and NaCl.

Spectral and Substrate-, Inhibitor-, and Heme Ligand-Binding Experiments for the nNOS Oxygenase Domain. All experiments in this study were carried out at 4 °C to minimize spectral changes of the proteins associated with their denaturation during prolonged incubation periods (up to 10 days). Stock solutions of L-Arg (500 mM), NNA (20 mM), NMA (20 mM), thiocitrulline (20 mM), DTT (0.1 and 1 M), and BME (1 M) were prepared in water, and those of BH_4 and 4-amino-BH_4 (10 mM) were made in water containing either 0.1 M DTT or 0.1 M BME. BH_2 was dissolved in dimethyl sulfoxide as a 20 mM stock solution. All of these solutions were stored in small aliquots (100−250 μL) at −70 °C. For anaerobic incubation experiments with the nNOS oxygenase domain, a small aliquot (25−30 μL) of concentrated protein stock solutions was diluted in argon-bubbled buffer (~300 μL) in a rubber septum-sealed cuvette (0.2 cm) by using a gastight microsyringe. While continuously purging oxygen by blowing argon into the cuvette, desired volumes (<35 μL) of stock solutions of compounds (substrate, pterins, etc.) were added to the sample, also by microsyringe. Preincubation of the nNOS oxygenase domain (~80 μM in 50 mM Tris buffer, pH 7.5) with DTT

[2] Presented at the 8th International Conference on Biological Inorganic Chemistry, Yokohama, Japan, July 27−August 1, 1997 (*61*).

(2.5 mM) was also performed under argon. Anaerobic stock solutions of easily autoxidizable compounds such as thiol-free BH_4, thiols (cysteine, glutathione), and ascorbate were prepared in argon-bubbled water (BH_4·2HCl, 10 mM), or in 50 mM potassium phosphate buffer, pH 6.8 (thiols, 100 mM), or in 100 mM sodium carbonate (ascorbic acid, 100 mM).

For typical spectral and titration experiments, the oxygenase domain (~100 μM) stock solution (containing 1 mM BME) was diluted to 10−20 μM in either 50 mM potassium phosphate (pH 6.5, 6.8, or 7.5) or 50 mM Tris (pH 7.5) buffer. The buffers contained 10% glycerol, 0.1 mM EDTA, and no BME. A 0.1 or 0.2 cm cuvette was used having a total volume of 150 or 300 μL, respectively. Equilibrium dissociation constants (K_d) for the ferric oxygenase domain complexes with heme ligands (imidazoles, cyanide, and DTT) were determined by spectrophotometric titrations. Data analysis was done by using double-reciprocal plots ($1/\Delta(\Delta A)$ vs $1/[L]$) of the resulting difference spectra in the Soret region (350−500 nm) using the equation: $1/\Delta(\Delta A) = K_d/\Delta(\Delta A_\infty)[L] + 1/\Delta(\Delta A_\infty)$, where [L] is the free ligand concentration and ΔA and ΔA_∞ are absorbance changes caused by ligand at $0 < [L] < \infty$ and $[L] = \infty$, respectively.

Preparation and Spectral Recording of the Half-Semiquinone Form of the nNOS Reductase Domain. To an aerobic solution of the ferricyanide-oxidized reductase domain (~120 μM, based on 2 mol of flavin/mol of domain: see below) in 50 mM potassium phosphate, pH 7.5, containing 10% glycerol and 0.1 mM EDTA was added NADPH (130 μM) at 4 °C. Upon this treatment, the absorbance of the oxidized reductase domain in the region >400 nm initially drastically decreased due to reduction of the flavins. The solution was then gently bubbled with ~20 μL of air using a microsyringe. The absorbance of the resulting reductase domain between 400 and 700 nm gradually increased with time (in ~20 min), as in the case of P450 reductase (*30*), to give a relatively stable neutral semiquinone spectrum having absorption bands at 590 and 630 nm, in addition to those at 456 and 476 nm.

Determination of Subunit-Based Protein Concentrations. The concentrations of full-length nNOS and the nNOS oxygenase domain were determined based on (1 heme/subunit protein) the pyridine hemochromogen assay (ϵ_{556} = 34 mM^{-1} cm^{-1}) (*29*). The concentration of ferricyanide-oxidized reductase domain (*23*) was determined based on 2 flavins/subunit protein using ϵ_{445} = 20.6 mM^{-1} cm^{-1} at pH 7.4 (*30*−*32*).

Optical Absorption and Magnetic Circular Dichroism (MCD) Spectroscopy. Electronic absorption spectra were recorded with a Varian/Cary 210 or 219 spectrophotometer interfaced to IBM PCs. MCD spectra were recorded with a Jasco J500A spectropolarimeter equipped with a Jasco MCD-1B electromagnet operated at 1.41 T. All spectral measurements were performed at ~4 °C using 0.1, 0.2, 0.5, or 1 cm quartz cuvettes (see ref *29*).

RESULTS

Spectral Properties and Complex Formation of the nNOS Oxygenase Domain with Substrate, Inhibitors, and Heme Ligands. The nNOS oxygenase domain used in this study was judged to be dimeric based on a gel filtration chromatogram at its final purification step.[3] The MCD and electronic absorption spectra of the BH_4-free ferric oxygenase domain

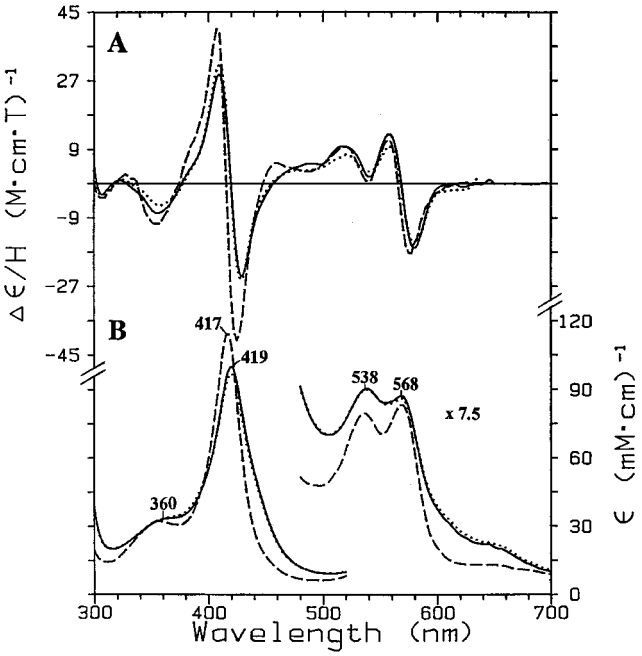

FIGURE 1: MCD (A) and electronic absorption spectra (B) of the BH_4-free ferric nNOS oxygenase domain and camphor-free ferric P450-CAM. The nNOS oxygenase domain in the absence (—) and presence of 10 mM L-Arg (···) and camphor-free P450-CAM (- - -). The spectra in the visible region (480−700 nm) are enlarged 7.5 times. The spectra of the nNOS oxygenase domain (10.8 μM) were recorded at 4 °C in 50 mM potassium phosphate buffer (pH 6.5) containing 10% (v/v) glycerol and 0.1 mM EDTA using 0.5 cm (MCD) and 0.2 cm (UV−visible) cuvettes. The spectra of P450-CAM are taken from ref *33*.

(the N-terminal amino acid residues 1−714) in the absence and presence of 10 mM L-Arg are shown in Figure 1, panels A and B, respectively, together with the spectra of camphor-free ferric P450-CAM (*33*). Both proteins exhibit very similar low-spin-type absorption and MCD spectra with respect to band positions and intensities, and spectral patterns. Given the fingerprinting capability of MCD spectroscopy (*29*, *34*), this indicates that the ferric oxygenase domain most likely has an [RS^-−Fe^{III}(heme)−OH_2] active site coordination sphere structure, where RS^- = Cys^--415 for nNOS (*23*, *35*), as does camphor-free P450-CAM (*34*, *36*). No detectable spectral differences were observed for the oxygenase domain in potassium phosphate buffer (pH 6.5 and 7.5) and Tris buffer (pH 7.5). Addition of the substrate L-Arg (10 mM) (Figure 1, dotted lines) or substrate analogue inhibitors (1 mM, NNA and NMA) (not shown) to the ferric oxygenase domain (Figure 1, solid lines) caused only very small spectral changes, if any, even after overnight incubation at 4 °C.

The ferric oxygenase domain forms low-spin complexes with heme ligands such as imidazoles (unsubstituted and substituted), cyanide, and DTT. These oxygenase domain complexes exhibit absorption and MCD spectra (not shown) very similar to those of the corresponding P450-CAM derivatives (*33*, *37*, *38*) in band positions, intensities, and spectral patterns. Similar MCD spectra (except for some differences in intensity) for the corresponding complexes

[3] The nNOS oxygenase domain expressed in *E. coli* and used in this study was primarily dimeric as judged by the final gel sizing column chromatogram (Hiload 26/60 Superdex 200 gel, Pharmacia). Shoulder fractions containing the monomer were excluded.

Table 1: Electronic Absorption Spectral Parameters and Dissociation Constants (K_d Values) for Heme Ligand Complexes of the Ferric nNOS Oxygenase Domain at 4 °C

	λ_{nm} ($\epsilon_{mM^{-1}\,cm^{-1}}$)					
	Soret		visible		K_d (mM)	
heme ligand[a]	δ	γ	β	α	pH 6.5[b]	pH 7.5[c]
none	360 (32)	419 (100)	538 (11.9)	568 (11.2)		
Imid	361 (35)	429 (92)	545 (12.3)	570[d] (9.4)	−	0.022
N-MeImid	361 (36)	429 (92)	545 (12.1)	570[d] (9.3)	0.13	0.038
cyanide	368 (40)	439 (69)	556 (11.2)		1.7	−
DTT	376 (56)	460 (57)	560 (13.6)		1.1	0.12

[a] Imid, imidazole; N-MeImid, *N*-methylimidazole; DTT, dithiothreitol. [b] 50 mM potassium phosphate containing 10% glycerol and 0.1 mM EDTA. [c] 50 mM Tris containing 10% glycerol and 0.1 mM EDTA. [d] Shoulder.

with imidazole and cyanide for full-length eNOS have also been recently reported (*39*). Absorption spectral data as well as dissociation equilibrium constants (K_d values) of four selected complexes are summarized in Table 1. All the imidazole derivatives examined in this study formed low-spin complexes with the ferric nNOS oxygenase domain which exhibit similar absorption spectra to one another. The observed pH dependence of the K_d values for the *N*-methylimidazole ($pK_a = 7.25$, see ref *40* for imidazoles) and DTT ($pK_a = 8.1$) complexes indicates that it is the unprotonated (neutral) form of *N*-methylimidazole and the deprotonated (anionic) form of DTT that coordinate to the ferric heme iron of the enzyme. Similar results have been previously reported for DTT binding to camphor-free P450-CAM (*38*). The K_d values of the complexes at pH 7.5 are similar for unsubstituted imidazole ($pK_a = 6.9$), *N*-phenylimidazole ($pK_a = \sim 5.85$, estimated) ($K_d = \sim 20$ μM for both), and *N*-methylimidazole ($K_d = 38$ μM). However, the affinity for 4-phenylimidazole ($pK_a = 6.0$) ($K_d = 0.69$ mM) is considerably lower (by >15-fold) than those for the others. Interestingly, while the 4-phenylimidazole complex is low-spin for the nNOS oxygenase domain, the analogous complex is high-spin for full-length eNOS (*39*) and nNOS (this study). The K_d value (=0.12 mM) of the DTT−oxygenase domain complex at pH 7.5 was either not affected ($K_d = 0.12$ mM) by 10 mM L-Arg or 1 mM NMA or somewhat affected ($K_d = 0.25$ mM) by 1 mM NNA.

Spectral Changes Due to Spin-State Conversion upon Binding of L-Arg, *Inhibitors, and* BH_4 *to the Ferric nNOS Oxygenase Domain*. Binding of L-Arg, its analogue inhibitors, or BH_4 to NOS has been shown to correlate with spectral (spin state) changes of the ferric enzyme by using radioisotope-labeled compounds for binding and spectrophotometric techniques for the spin-state changes (*17*, *24*, *41*, *42*).[4] Individual addition of either the substrate L-Arg (10 mM) or its analogue inhibitors NNA and NMA (1 mM), or BH_4 (0.25 mM), to the low-spin ferric oxygenase domain did not cause readily detectable spin-state conversion of the heme iron even after incubation for 2 days at 4 °C under aerobic conditions. However, when BH_4 (0.25 mM) was added together with DTT (2.5 mM) either in the presence or in the absence of L-Arg, NNA, or NMA, noticeable, although quite

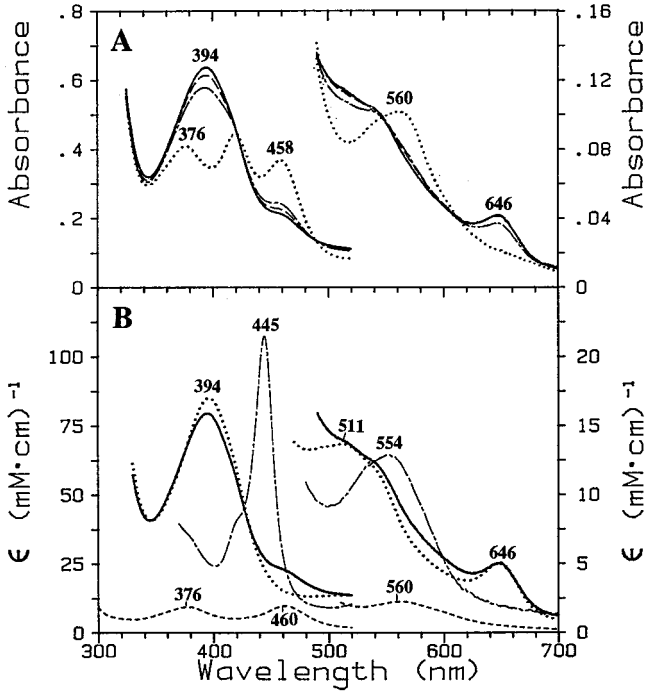

FIGURE 2: (A) Electronic absorption spectral changes of the ferric nNOS oxygenase domain (16.9 μM) from a low-spin to high-spin type after addition of 2 mM L-Arg, 0.25 mM BH_4, and 2.5 mM DTT as a function of incubation time. The spectra were recorded using a 0.5 cm cuvette after incubation for 0 h (• • •), 24 h (− • −), 42 h (- - -), and 70 h (—). See the legend to Figure 1 for other conditions. (B) Normalized electronic absorption spectra of the incubated (70 h) nNOS oxygenase domain as described in panel A before (—) and after (• • •) subtraction of a fractional (15%) spectrum of the DTT complex (- - -). The spectrum of the dithionite-reduced ferrous-CO form (− • −) of the same incubated nNOS oxygenase domain sample is also shown.

slow, spectral changes were observed during prolonged incubation at 4 °C. Figure 2A displays representative results where, upon concomitant addition of L-Arg (2 mM) and BH_4 (0.25 mM) together with DTT (2.5 mM) at pH 6.5, the low-spin-type absorption spectrum of the oxygenase domain (see Figure 1B, solid line) was initially quickly (<30 s) converted to that of a partially (~70%, $K_d = 1.1$ mM) DTT-bound form (Figure 2A, dotted line). During the next hour, only a small spectral change was observed (not shown). After incubation for 24 h at 4 °C, the spectrum changed considerably to that of a high-spin-type (dot−dashed line) having major peaks at ~395 and ~650 nm. Upon further incubation for a total of 42 h (long dashed line), the intensity of the two peaks increased further and reached a near-maximum value in ~70 h (solid line). During the spectral change, only

[4] Recent crystal structural analysis of the BH_4- and/or L-Arg-bound dimeric oxygenase domains of iNOS and eNOS indicates that there is a close linkage, through an extensive hydrogen bond network, between pterin/substrate binding and formation of the five-coordinate (high-spin) heme (see refs *12*−*15* for details). Thus, it is unlikely that BH_4 and/or L-Arg could bind to the low-spin NOS oxygenase domain without perturbing the spectrum of the heme in the oxygenase domain.

one set of isosbestic points was observed. The resulting spectrum still has a small band at ~460 nm which is attributable to a small amount of the DTT complex of the ferric oxygenase domain. Similar spectral conversion results were obtained at pH values of 6.8 (phosphate) and 7.5 (Tris or phosphate) to those at pH 6.5 (phosphate) except that at pH 7.5 the ferric nNOS oxygenase domain was almost completely (~95%, $K_d = 0.12$ mM) saturated with 2.5 mM DTT at the initial stage of incubation.

To obtain the spectrum of the DTT-free oxygenase domain of the incubated sample, we arithmetically subtracted fractions (10−20%) of the spectrum of the DTT−oxygenase domain complex from the spectrum of the incubated sample obtained at pH 6.5 (Figure 2B, solid line). Spectral subtraction of 15% of the DTT complex (spectrum with 15% intensity plotted in Figure 2B, short dashed line) completely removed the band at ~460 nm. This yielded an absorption spectrum typical of a high-spin ferric heme with a Soret band at 394 nm and visible region bands at ~512 and 646 nm (Figure 2B, dotted line). The integrity of the incubated oxygenase domain was ensured by converting it to dithionite-reduced deoxyferrous species [spectrum not shown, $\lambda_{max,\ nm}$ ($\epsilon_{mM^{-1}\ cm^{-1}}$): 412 (74), 555 (13.6)] and then, by CO bubbling, to the ferrous-CO form. Both of these forms exhibited electronic (Figure 2B, dot−dashed line, for the latter) and MCD (not shown) spectra that are very similar to those of the corresponding states of intact nNOS (*29*).

Moreover, the high-spin ferric oxygenase domain, generated as described above by prolonged incubation in the presence of L-Arg (2 mM), BH_4 (0.25 mM), and DTT (2.5 mM), readily binds potassium cyanide to exhibit absorption bands at ~364, 439, and ~562 nm (spectrum not shown). The cyanide affinity ($K_d = \sim 10$ mM) of the high-spin nNOS oxygenase domain thus generated is somewhat lower than that ($K_d = 1.7$ mM) of the BH_4- and L-Arg-free low-spin oxygenase domain. But the K_d value is similar to that ($K_d =$ 6−8 mM) of pterin- and substrate-bound full-length nNOS in the absence of Ca^{2+}-calmodulin (*43*, this work).

The MCD spectrum of the L-Arg-bound ferric high-spin oxygenase domain thus generated after subtraction of the spectrum (15%) of the DTT complex has a spectral band pattern (spectrum not shown) that is similar to that of L-Arg-bound full-length ferric nNOS (*29*). Their MCD spectra are characteristic of thiolate-ligated five-coordinate ferric high-spin heme complexes (*34*). The nNOS reductase domain (half semiquinone or fully oxidized) exhibits a very small MCD signal ($|\Delta\epsilon/H| \leq 1\ M^{-1}\ cm^{-1}\ T^{-1}$) in the 300−700 nm region (this work).

When the inhibitors NNA and NMA were used in place of Arg, together with BH_4 and DTT, a similar low-spin to high-spin spectral conversion also occurred for the ferric oxygenase domain as shown in Figure 3A (NNA) and 3B (NMA). Subtractions of 10% (for NNA) and 15% (for NMA) of the DTT−oxygenase domain complex spectrum yielded typical high-spin-type spectra for both inhibitors. Noticeably, the absorption band positions for the NNA−oxygenase domain adduct (λ_{max}: 401, 516, 650 nm) are slightly but detectably red-shifted from those of the NMA and L-Arg adducts (λ_{max}: 394, ~512, 646 nm for both adducts).

The spectrum of the nNOS oxygenase domain in the presence of BH_4 (0.25 mM) and DTT (2.5 mM), but without L-Arg or the inhibitors, also resulted in a low-spin to high-spin spectral change as displayed in Figure 3C (dashed line). However, the maximum extent of formation of the high-spin species after 6 days incubation in this case (see a high-spin marker band at 644 nm) was somewhat smaller than those in the presence of the substrate or inhibitors. After subtraction of 20% of the spectrum of the DTT−oxygenase domain complex, the resulting spectrum (solid line in Figure 3C) accounts for ~70% high-spin. Thus, in this case, the overall distribution is ~20% DTT complex (BH_4-free), ~55% high-spin (DTT-free, BH_4-bound) species, and ~25% low-spin (DTT-free, BH_4-bound) species. Such detailed estimation (±5%) of low (high)-spin fractions for the ferric nNOS oxygenase species is possible because of the successful conversion of the ferric nNOS oxygenase domain in this study from its nearly completely (≥95%) low-spin to high-spin (≥95%) form. The estimation was done by simulation of the absorption spectrum (300−500 nm) by arithmetically

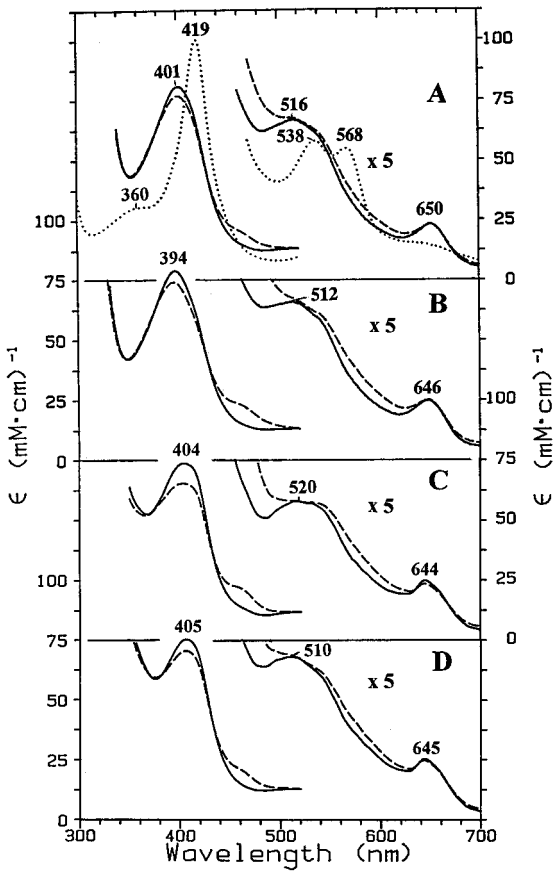

FIGURE 3: BH_4/DTT-induced low-spin to high-spin spectral changes of the ferric nNOS oxygenase domain (10−17 μM) after prolonged incubation for 2−6 days in the presence and absence of various inhibitors. Panel A, with 0.5 mM N^G-nitro-L-Arg (NNA); panel B, with 0.5 mM N^G-methyl-L-Arg (NMA); panel C, with BH_4/DTT alone; panel D, after addition of 2 mM L-thiocitrulline to panel C and further incubation for 24 h. Plotted are the spectra of the nNOS oxygenase domain before (• • •, panel A only) and after (− −) addition of and prolonged incubation with 0.25 mM BH_4, 2.5 mM DTT, and the various inhibitors. All spectra in the visible region (460−700 nm) are enlarged 5 times. The incubation was carried out for 69−72 h (~3 days) for panels A and B and for ~6 days for panel C in 50 mM potassium phosphate (pH 6.5 for panels A and B, pH 6.8 for panels C and D) at 4 °C. Solid line spectra (—) are obtained after subtraction (from the dashed line spectra) and normalization for 10% (A), 15% (B), 20% (C), and 15% (D) of the oxygenase domain−DTT complex spectrum. In panel D, the spectral change upon addition of L-thiocitrulline was nearly complete within 1 min.

Table 2: Effects of L-Arg (or NMA or NNA), Pterins (BH_4, BH_2), Thiols, Imidazole, and Ascorbic Acid on the Low-Spin to High-Spin Conversion of Ferric nNOS Oxygenase Domain upon Incubation at pH 6.5−6.8 and 4 °C in 50 mM Potassium Phosphate Containing 10% (v/v) Glycerol and 0.1 mM EDTA

compound(s) added[a]	conversion to high-spin[b] (max conversion)	rel conversion rate (time required for 50% of max conversion)
L-Arg	no	
DTT	no	
BH_4[c,d]	no	
BH_4 + DTT	yes (∼70%)	very slow (1.5−2 days)
L-Arg + BH_4[c,d]	no	
L-Arg + DTT	yes (∼80%)	very slow (1.5−2 days)
L-Arg (or NMA or NNA) + BH_4 + DTT	yes (≥95%)	slow (∼10 h)
L-Arg + BH_4 + BME	yes (∼90%)	slow (15−20 h)
L-Arg (or NMA) + BH_2 + DTT	yes (≥95%)	slow (∼15 h)
L-Arg (or NMA) + BH_2	no	
BH_2	no	
BH_2 + DTT	yes (∼70%)	very slow (2−3 days)
imidazole	no	
imidazole + L-Arg + BH_2	no	
imidazole + L-Arg + BH_2 + DTT	yes (∼90%)	very slow (1.5−2 days)
L-Arg + BH_2 + cysteine[c]	yes (∼70%)	very slow (1.5−2 days)
L-Arg + BH_2 + glutathione[c]	yes (∼70%)	very slow (1.5−2 days)
L-Arg + BH_2 + ascorbic acid[c,d]	no	

[a] With 0.5 or 2.5 mM L-Arg (or 0.5 mM NMA and NNA), 0.25 mM (aerobic) or 1 mM (anaerobic) BH_4, 0.15 mM BH_2, 2.5 mM DTT, 10 mM BME, 1 mM imidazole, 10 mM cysteine, glutathione, or ascorbic acid. [b] No: no detectable spectral changes observed in 2 days. The "very slow" conversion was monitored for 10 days for glutathione and cysteine and for 6−7 days for the others. No detectable precipitation or denaturation (examined by conversion to the dithionite-reduced CO form) of the samples was observed even after prolonged incubation at 4 °C. The percent high-spin fractions are estimated after subtraction of the remaining DTT or BME complex (see text for details, no spectrally detectable complex formation observed with the other thiols). [c] Under anaerobic conditions (argon atmosphere). [d] Catalase (0.1 mg/mL) was added to prevent any effects of adventitiously produced H_2O_2.

combining the spectra of the low-spin (Figure 1B, solid line, or Figure 3A, dotted line) and high-spin (Figure 2B, dotted line) nNOS oxygenase domains in various ratios.

Addition of another competitive inhibitor, thiocitrulline (1 mM) (*44*), to the above BH_4/DTT-containing ferric oxygenase domain sample (solid line in Figure 3C), followed by further incubation for ∼24 h at 4 °C, converted it to another predominantly high-spin-type species (Figure 3D, dashed line). The resulting species exhibits an absorption spectrum that is distinguishable from the spectrum of the thiocitrulline-free species in the ∼405 nm (narrower band for the thiocitrulline complex) and ∼510 nm (more intense band for the complex) regions. Subtraction of 15% of the DTT−oxygenase domain complex spectrum (Figure 2B, dashed line) gave an apparently DTT-free predominantly (∼75%) high-spin-type absorption spectrum (Figure 3D, solid line) which has a considerably more red-shifted Soret band than those for the L-Arg, NNA, and NMA complex. (Overall 15% DTT complex, ∼65% high-spin species, and ∼20% low-spin species; the latter two are DTT-free and thiocitrulline-bound.) The complexes of ferric nNOS with L-Arg and these inhibitors were also shown to exhibit electron paramagnetic resonance spectra that are distinguishable from one another (*45*).

For all of the cases described above, the resulting spectra (after DTT complex subtraction) minus the starting low-spin spectrum of the ferric oxygenase domain exhibited difference spectra (not shown) having a peak at ∼390 nm and a trough at ∼420 nm. These so-called type-1 difference spectra (observed with P450 enzymes upon substrate binding) (*46*) have varying peak-to-trough intensities [$\Delta(\Delta\epsilon_{peak} - \Delta\epsilon_{trough})$] depending on the compound used. The $\Delta(\Delta\epsilon_{peak} - \Delta\epsilon_{trough})$ value for the nNOS oxygenase domain ± L-Arg was 86 mM^{-1} cm^{-1} (cf. 120 mM^{-1} cm^{-1} for P450-CAM ± camphor).

In the experiments described above, BH_4 was used always in combination with DTT because BH_4 stock solutions (10 mM) were prepared in 100 mM DTT to maintain the pterin in its reduced form. To understand the roles of BH_4 and DTT in the heme spin conversion of the ferric nNOS oxygenase domain, the effects of each of these compounds as well as those of other compounds on the absorption spectral change of the domain were further investigated. Those compounds include BH_2 (an autoxidation product of BH_4), other thiols (cysteine and glutathione), imidazole (heme ligand), and ascorbate (reductant). They were used individually or in combination with others. Results are summarized in Table 2. The most noteworthy finding is that a thiol is essential for the heme spin conversion to occur. Even though any of these individual thiols alone was apparently ineffective (however, see below for preincubation effects), their use in combination with substrate (or its analogue inhibitor) and/or BH_4 (or BH_2) did induce a spectral change of the nNOS oxygenase domain from a low-spin to high-spin type. Of all the conditions examined, we found that a combination of substrate (or its analogue inhibitors), BH_4, and DTT exhibited the fastest rate of spectral change (with an apparent $t_{1/2}$ of ∼10 h) and the largest extent (≥95%) of conversion to high-spin state. Note that L-Arg plus pterin did not induce spin conversion of the imidazole complex unless DTT was added. Among the four thiols used, DTT was considerably more effective than the others.

We also found significant acceleration of the spin-state conversion of the nNOS oxygenase domain when it had been preincubated with DTT. For example, preincubation of the nNOS oxygenase domain with 2.5 mM DTT for 2 days at 4

°C under argon led to an increase in the spin-state conversion rate by more than 2-fold. Thus, the $t_{1/2}$ values for the preincubated oxygenase domain containing BH_4/DTT or L-Arg/BH_4/DTT were 10−15 and ∼5 h, respectively. In addition, for the former case, the maximum extent of the spin-state conversion increased from ∼70% (without preincubation) to ∼90%.

Furthermore, somewhat unexpectedly, BH_4 alone (even at 1 mM) or in combination with L-Arg is incapable of changing the heme spin state even under anaerobic conditions (argon) where autoxidation of BH_4 was carefully prevented. When the absorption spectrum of BH_4 [λ_{max}: 296 nm, ϵ = 8.8 mM^{-1} cm^{-1} at pH 6.8 (*47*)] was monitored between 255 and 400 nm, only about 15% of BH_4 was autoxidized to BH_2 at the end of 35 h anaerobic incubation of the nNOS oxygenase sample. BH_2 exhibits λ_{max} of 279 and 328 nm (this work for the latter) with ϵ = 12.7 and 6.8 mM^{-1} cm^{-1} at pH 6.8 (*47*), respectively. The sample in this work contained 1 mM pterin and 2.5 mM L-Arg at pH 6.8 and 4 °C. During the incubation, no detectable spectral change of the oxygenase domain was observed. In these experiments, the spectral change of the oxygenase domain and that of BH_4 were monitored in the 400−750 nm region (where BH_4 and BH_2 do not absorb) and 255−400 nm region (after subtracting the oxygenase domain absorption), respectively. In control experiments where the autoxidation of BH_4 to BH_2 was monitored under similar conditions for longer incubation time without the enzyme, no spectrally detectable intermediates were observed during the autoxidation process. Similarly, 4-amino-BH_4, a potent antagonist of BH_4 (*17*), in combination with L-Arg, did not induce a low-spin- to high-spin-type spectral change in the nNOS oxygenase domain without DTT. 4-Amino-BH_4 (λ_{max}: 293 nm at pH 6.8, this work) is also readily autoxidizable (λ_{max}: 291 and 328 nm for the oxidized product, $t_{1/2}$ = ∼40 min at pH 6.8 and 4 °C under air, this work). It effectively converted the heme spin state of the nNOS oxygenase domain when it was added in combination with DTT and L-Arg either in its reduced form [as is the case of full-length BH_4-free iNOS (*17*)] or in its oxidized form (data not shown).

Spectral Reconstruction of Native Intact Ferric nNOS from Its Separated Oxygenase and Reductase Domains. Native intact ferric nNOS has been shown to contain a neutral semiquinone radical species that is air-stable and detected with electron paramagnetic resonance spectroscopy (*28*). In this work the semiquinone form of the nNOS reductase domain (residues 715−1429) was generated by aerobic reduction of the ferricyanide-oxidized domain (dotted line, Figure 4A) with NADPH. The absorption spectrum of the resulting semiquinone form (dot−dashed line, Figure 4A) has prominent bands at ∼592 and ∼630 nm with extinction coefficient (ϵ) values of 4.3 and 3.9 mM^{-1} cm^{-1}, respectively. These spectral features are in reasonable agreement, in both the band positions and intensities, with those of the corresponding state of the yeast-expressed nNOS reductase domain (*48*), the baculovirus-expressed heme-deficient Cys415Ala mutant of full-length nNOS (*35*), and microsomal P450 reductase (*30*−*32*).

The absorption band intensity at 640−650 nm (high-spin marker band) of reductase domain-containing, Arg-bound full-length ferric NOS (ϵ = 7.5−8 mM^{-1} cm^{-1}) (solid line in Figure 4B) is noticeably greater that those (ϵ = ∼5 mM^{-1} cm^{-1}) of the other two thiolate-ligated ferric heme proteins P450 and chloroperoxidase (*29*). This unusual spectral feature of native intact NOS was lost (ϵ_{645} decreased to ∼5 mM^{-1} cm^{-1}) when the ferric enzyme was oxidized with ferricyanide, and reappeared by stoichiometric anaerobic reduction with NADPH (*28, 35, 48*).[5] The UV−visible absorption spectrum of L-Arg-bound ferric full-length nNOS is reasonably well simulated by arithmetically combining the spectrum of the BH_4- and L-Arg-bound high-spin oxygenase domain with the spectrum of the reductase domain containing one flavin neutral semiquinone and one oxidized flavin (dot−dashed line in Figure 4B). Although spectral reconstruction has previously been reported for trypsin-cleaved full-length iNOS (*7*), this study provides a stoichiometrically more accurate spectral reconstruction by using the separately expressed oxygenase and reductase domains of nNOS. Thus, the substrate-bound, fully heme- and flavin-saturated full-

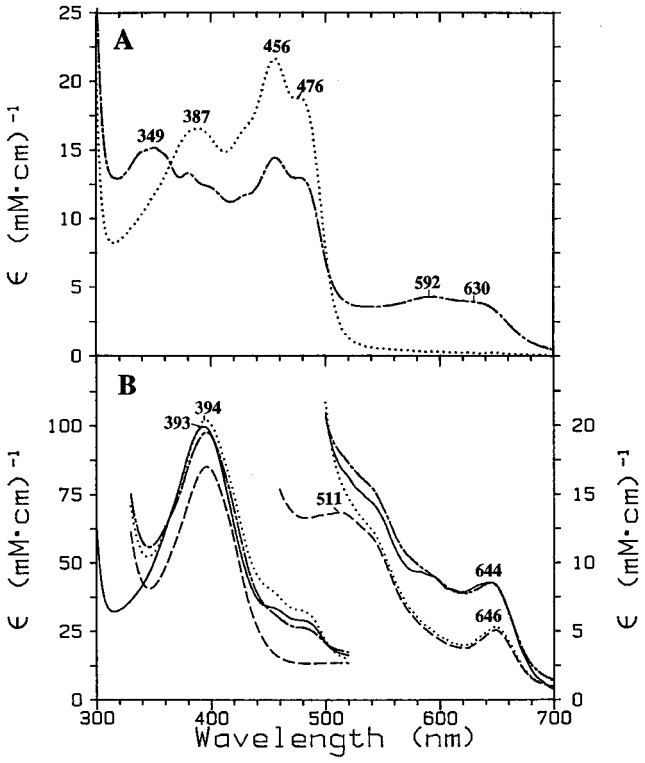

FIGURE 4: Reconstruction of the electronic absorption spectrum of native full-length L-Arg-bound ferric nNOS from the spectrum of the L-Arg/BH_4/DTT-induced high-spin state of the nNOS oxygenase domain and that of the reductase domain containing one semiquinone moiety and one oxidized flavin moiety (i.e., a half-semiquinone form). Panel A: absorption spectra of the reductase domain of nNOS before (· · ·) and after (− · −) its aerobic reduction with NADPH to the half-semiquinone form. The half-semiquinone form was prepared as described under Experimental Procedures. Panel B: absorption spectra of the L-Arg/BH_4/DTT-induced and DTT complex-subtracted (15%) high-spin form of the nNOS oxygenase domain (- - -) plus the spectrum of the ferricyanide-oxidized reductase domain (combined spectrum, · · ·) or plus that of the half-semiquinone form of the reductase domain (combined spectrum, − · −). The spectrum of BH_4-containing recombinant full-length L-Arg-bound ferric nNOS (—) newly recorded in this study (cf. ref *29*) is also overplotted.

[5] Air-oxidation by incubation overnight at 4 °C of the dithionite-reduced, ferrous-CO form of native full-length L-Arg-bound nNOS also yielded high-spin ferric enzyme exhibiting a low absorption intensity (ϵ = ∼5 mM^{-1} cm^{-1}) at ∼650 nm, i.e., the enzyme having completely oxidized flavins (this work).

length ferric NOS has an A_{450}/A_{393} value no greater than 0.35, and the reductase domain flavin groups contribute to the total absorbance for the Soret band of the enzyme ($\epsilon_{393} = \sim 100$ mM^{-1} cm^{-1}) by about 12.5% (or $\Delta\epsilon = 12.5$ mM^{-1} cm^{-1}).

DISCUSSION

Effects of BH_4 on the Absorption Spectrum and Spin State of Ferric NOS and on Binding of Heme Ligands to the Enzyme. Unlike the majority of the P450 isoforms, the three full-length BH_4-containing ferric NOS isoforms are all predominantly (≥80%) five-coordinate high-spin ($\lambda_{max} = \sim 400$ and ~650 nm) even in the absence of the substrate L-Arg (*8*, *28*, *29*). Both ferric intact NOS (*24*, *43*, *49*) and P450 (*33*, *50*) form complexes with several types of heme ligands including imidazole, cyanide, and pyridine. In contrast to P450 (*38*, *50*), however, substrate-free full-length ferric NOS does not readily bind DTT (*51*), unless NOS is also BH_4-free. Thus, DTT only gains access to the active site of BH_4-free full-length dimeric nNOS and forms bis-thiolate adducts with the ferric heme iron, exhibiting unique split Soret (or "hyperporphyrin") spectra with absorption bands at ~380 and ~460 nm (*38*, *52*). The active site of intact BH_4-containing ferric iNOS has also been shown to become accessible to DTT upon addition of the denaturant urea in molar concentrations. This was attributed to dimer to monomer conversion of full-length iNOS (*51*), which is accompanied by dissociation of the enzyme-bound BH_4. BH_4 also stabilizes the dimeric structure of full-length nNOS (*16*, *41*) and iNOS (*17*), but apparently not for eNOS (*8*), although the enzymes are largely (>80%) dimeric in their BH_4-free forms (*8*, *13*, *41*, *53*) in these cases.

Requirement of DTT for Binding of BH_4 and L-Arg *to NOS and for Catalytic Function of NOS.* The most striking finding in this study is that neither BH_4 nor L-Arg readily binds to the nNOS oxygenase domain unless a thiol (e.g., DTT) at 2.5−10 mM is present. Low concentrations (0.1−0.2 mM) of BME that had been brought in from the stock solutions of the nNOS oxygenase domain had little effect. Moreover, only in the presence of DTT, BH_2 (a BH_4 autoxidation product which is not reducible with DTT) can also bind to the oxygenase domain (Table 2). Stuehr, Mayer, and their co-workers have reported that, in the case of the pterin-free iNOS oxygenase domain, BH_2 can bind to the protein in competition with BH_4 with somewhat lower affinity than BH_4 (*42*). More recently, Stuehr's group has demonstrated that BH_2 and several other pterin derivatives can induce spin-state conversion of full-length iNOS as well as its separated oxygenase domain to similar extents to those caused by BH_4 (*53*), despite the fact that BH_2 cannot support the NOS catalysis (*53*). Again their buffer contained 1 mM DTT or 2.5 mM BME. Based on these results, we propose that DTT (and other thiols), in addition to maintaining the pterin in the reduced form (i.e., BH_4), plays a crucial role(s) in converting the BH_4-free nNOS oxygenase domain from a form which is inaccessible to BH_4 and/or L-Arg to an accessible form.

A thiol (DTT or BME in 1−2.5 mM) is always included in a standard NOS assay mixture. Many thiols (also including glutathione and cysteine) are known to dramatically enhance the catalytic activity of purified NOS by up to severalfold in dose- and preincubation time-dependent manners (*52*, *54*, *55*). These effects of thiols are explained by (a) their ability to maintain BH_4 in its catalytically active reduced form (*54*−*56*) and, in part, by (b) possible reductive protection of the NOS protein (*52*, *55*). However, it should be emphasized that these previous studies have not specifically examined the requirement of a thiol for binding of BH_4 and/or L-Arg to either BH_4-free full-length NOS or BH_4-free NOS oxygenase domain as we have done in this study for the nNOS oxygenase domain. The present study clearly rules out the BH_4-regenerating role of DTT for its requirement. Since the nNOS oxygenase domain used in this study was judged to be dimeric vide supra,[3] DTT does not appear to be required simply for dimerization of the domain for the binding of the pterin and/or substrate. However, the thiol requirement for BH_4 and/or L-Arg binding as well as the significant binding rate acceleration by preincubation with DTT are suggestive of protein cysteine group involvement in the restoration of the pterin- and substrate-binding capability of the separated domain. Relevant to this proposal, recent crystallographic as well as cysteine residue point mutation studies by several research groups are described below.

Recently, Masters, Poulos, and co-workers (*13*) and, shortly afterward, Fischmann and co-workers (*14*) have determined the X-ray crystal structures of the dimeric eNOS and iNOS (and also nNOS[6]) oxygenase domains. The eNOS (and nNOS[6]) oxygenase domain used by the former group was prepared by trypsin cleavage of the *E. coli*-expressed full-length enzyme (*13*). The structures for both isoforms revealed the presence of a $Zn(Cys)_4$ metal center at the dimer interface which involves two conserved cysteine groups (Cys101 and Cys96 for eNOS) and is likely important for the stability of the protein dimeric structure as well as the binding of BH_4 and L-Arg to the protein (*13*, *14*). It should be pointed out that both of these research groups crystallized the BH_4- and L-Arg-bound oxygenase domains under reducing conditions using tris(2-carboxyethyl)phosphine (*13*), glutathione sulfonate (*13*), or DTT (*14*). When zinc is absent, one of the thiol ligands (Cys101 in bovine eNOS, Cys99 in human eNOS, Cys109 in murine iNOS, and Cys331 in rat brain nNOS) is proposed to form an intersubunit disulfide bond (*13*). Crane, Stuehr, and co-workers (*12*) first detected such a disulfide bond in the murine iNOS oxygenase domain dimer structure. In fact, Poulos and collaborators have quite recently demonstrated that either the disulfide bond-containing or the $Zn(Cys)_4$ metal center-containing (with added $ZnSO_4$ and a reducing agent) structure can be prepared for the human iNOS oxygenase domain under different crystallization conditions (*15*).

Other laboratories had shown earlier that the Cys99Ala mutant of human eNOS (*57*) and the Cys109Ala mutant of murine iNOS (*42*) had partially impaired BH_4-binding capabilities. As isolated, these mutants gained ~20% and ~70% of the full catalytic activity of the wild-type enzymes, respectively, when sufficiently high concentrations (>100 μM) of BH_4 were added. Further, Masters and co-workers have recently demonstrated that the full-length Cys331Ala nNOS mutant is largely low-spin and defective in L-Arg binding and catalysis (*58*). However, prolonged (~12h at 4 °C) incubation of the mutant in the presence of a relatively

[6] C. S. Raman, H. Li, T. L. Poulos, P. Martásek, and B. S. S. Masters, unpublished observations.

high concentration of L-Arg (10 mM), with or without BH_4 (300 μM), has restored the high-spin-type absorption spectrum. More significantly, the full catalytic activity (with 10 μM BH_4) was also restored for the L-Arg-incubated mutant even in the absence of the enzyme-bound zinc (*58*, *59*). The Cys331Ala nNOS mutant lacks Zn-binding capability (*59*). Thus, Zn is not essential for catalysis.

In view of these recent findings, the thiol-assisted restoration of the pterin- and substrate-binding capability of the *E. coli*-expressed nNOS oxygenase domain might be related to the reductive cleavage or rearrangement of the intersubunit disulfide bond. The bond most likely involves either one or both of the two conserved cysteine groups (Cys331 and Cys326 for nNOS), as detected by X-ray crystallography for the homologous residue in iNOS (Cys109) (*12*, *15*). In the present case, zinc does not appear to be playing a crucial role; the zinc content in the *E. coli*-expressed nNOS oxygenase domain preparation has been shown to be less than stoichiometric (i.e., 0.2 mol/mol of dimer = 0.1 mol/mol of heme) (*59*). In addition, any zinc that might be inadvertently contained in the buffer used would be unavailable for the oxygenase domain because EDTA (0.1 mM), which is added to the buffer, would remove the free zinc. We have recently found that the DTT-assisted restoration of the BH_4- and substrate-binding capability of the nNOS oxygenase domain is essential for generation of a stable dioxygen complex of the dithionite-reduced nNOS oxygenase domain in 50% (v/v) ethylene glycol at −30 °C (*60*).

In conclusion, this study has demonstrated that a thiol, DTT in particular, is essential for the binding of BH_4 and L-Arg to the *E. coli*-expressed pterin-free ferric nNOS oxygenase domain. Thus, in the separate oxygenase domain, we have been able to generate a heme iron center that is spectroscopically identical to the full-length ferric nNOS active site structure having a five-coordinate high-spin ferric heme. This work will facilitate future studies aimed at achieving a better understanding of the significance of the unique cysteine-involving dimeric conformation of the NOS oxygenase domain and its active site structure, which have been recently revealed by X-ray crystallography (*12*−*15*).

ACKNOWLEDGMENT

We thank Drs. Edmund W. Svastits and John J. Rux for developing the computer-based spectroscopic data-handling system and Dr. John W. Ledbetter (Medical University of South Carolina) for his generous gift of BH_2.

REFERENCES

1. Marletta, M. A. (1994) *Cell 78*, 927−930.
2. Bredt, D. S., and Snyder, S. H. (1994) *Annu. Rev. Biochem. 63*, 175−195.
3. Griffith, O. W., and Stuehr, D. J. (1995) *Annu. Rev. Physiol. 57*, 707−736.
4. Moncada, S., and Higgs, E. A. (1995) *FASEB J. 10*, 1319−1330.
5. Masters, B. S. S., McMillan, K., Sheta, E. A., Nishimura, J. S., Roman, L. J., and Martasek, P. (1996) *FASEB J. 10*, 552−558.
6. Brenman, J. E., Chao, D. S., Gee, S. H., McGee, A. W., Craven, S. E., Santillano, D. R., Wu, Z., Huang, F., Xia, H., Peters, M. F., Froehner, S. C., and Bredt, D. S. (1996) *Cell 84*, 757−767.
7. Baek, K. J., Thiel, B. A., Lucas, S., and Stuehr, D. J. (1993) *J. Biol. Chem. 268*, 21120−21129.
8. Rodríguez-Crespo, Gerber, N. C., and Ortiz de Montellano, P. R. (1996) *J. Biol. Chem. 271*, 11462−11467.
9. Klatt, P., Pfeiffer, S., List, B., Lehner, D., Glatter, O., Bächinger, H. P., Werner, E. R., Schmidt, K., and Mayer, B. (1996) *J. Biol. Chem. 271*, 7336−7342.
10. Abu-Soud, H. M., and Stuehr, D. J. (1993) *Proc. Natl. Acad. Sci. U.S.A. 90*, 10769−10772.
11. Narhi, L. O., and Fulco, A. J. (1987) *J. Biol. Chem. 262*, 6683−6690.
12. Crane, B. R., Arvai, A. S., Ghosh, D. K., Wu, C., Getzoff, E. D., Stuehr, D. J., and Tainer, J. A. (1998) *Science 279*, 2121−2126.
13. Raman, C. S., Li, H., Martásek, P., Kral, V., Masters, B. S. S., and Poulos, T. L. (1998) *Cell 95*, 939−950.
14. Fishmann, T. O., Hruza, A., Niu, X. D., Fossetta, J. D., Lunn, C. A., Dolphin, E., Prongay, A. J., Reichert, P., Lundell, D. J., Narula, S. K., and Weber, P. C. (1999) *Nat. Struct. Biol. 6*, 233−242.
15. Li, H., Raman, C. S., Glaser, C. B., Blasko, E., Young, T. A., Parkinson, J. F., Whitlow, M., and Poulos, T. L. (1999) *J. Biol. Chem. 274*, 21276−21284.
16. Klatt, P., Schmidt, K., Lehner, D., Glatter, O., Bächinger, H. S., and Mayer, B. (1995) *EMBO J. 14*, 3687−3696.
17. Mayer, B., Wu, C., Gorren, A. C. F., Pfeiffer, S., Schmidt, K., Clark, P., Stuehr, D., and Werner, E. R. (1997) *Biochemistry 36*, 8422−8427.
18. Rusche, K. M., Spiering, M. M., and Marletta, M. A. (1998) *Biochemistry 37*, 15503−15512.
19. Perry, J. M., and Marletta, M. A. (1998) *Proc. Natl. Acad. Sci. U.S.A. 95*, 11101−11106.
20. Kaufman, S. (1997) *Tetrahydrobiopterin*: *Basic Biochemistry and Role in Human Disease*, The Johns Hopkins University Press, Baltimore, MD.
21. Kappock, T. J., and Caradonna, J. P. (1996) *Chem. Rev. 96*, 2659−2756.
22. Bec, N., Gorren, A. C. F., Voelder, C., Mayer, B., and Lange, R. (1998) *J. Biol. Chem. 273*, 13502−13508.
23. McMillan, K., and Masters, B. S. S. (1995) *Biochemistry 34*, 3686−3693.
24. Roman, L. J., Sheta, E. A., Martásek, P., Gross, S. S., Liu, Q., and Masters, B. S. S. (1995) *Proc. Natl. Acad. Sci. U.S.A. 92*, 8428−8452.
25. Martásek, P., Liu, Q., Liu, J., Roman, L. J., Gross, S. S., Sessa, W. C., and Masters, B. S. S. (1996) *Biochem. Biophys. Res. Commun. 219*, 359−365.
26. Wu, C., Zhang, J., Abu-Soud, H., Ghosh, D. K., and Stuehr, D. J. (1996) *Biochem. Biophys. Res. Commun. 222*, 439−444.
27. Thöny, B., Leimbacher, W., Bürgisser, D., and Heizmann, C. W. (1992) *Biochem. Biophys. Res. Commun. 189*, 1437−1443.
28. Stuehr, D. J., and Ikeda-Saito, M. (1992) *J. Biol. Chem. 267*, 20547−20550.
29. Sono, M., Stuehr, D. J., Ikeda-Saito, M., and Dawson, J. H. (1995) *J. Biol. Chem. 270*, 19943−19948.
30. Iyanagi, T., and Mason, H. S. (1973) *Biochemistry 12*, 2297−2308.
31. Masters, B. S. S., Kamin, H., Gibson, Q. H., and Williams, C. H., Jr. (1965) *J. Biol. Chem. 240*, 921−931.
32. Vermilion, J. L., and Coon, M. J. (1978) *J. Biol. Chem. 253*, 2694−2704.
33. Dawson, J. H., Andersson, L. A., and Sono, M. (1982) *J. Biol. Chem. 257*, 3606−3617.
34. Dawson, J. H., and Sono, M. (1987) *Chem. Rev. 87*, 1255−1276.
35. Richards, M. K., Clague, M. J., and Marletta, M. A. (1996) *Biochemistry 35*, 7772−7780.
36. Poulos, T. L., Finzel, B. C., and Howard, A. J. (1987) *J. Mol. Biol. 195*, 687−700.
37. Dawson, J. H., Andersson, L. A., Sono, M., and Hager, L. P. (1992) *New J. Chem. 16*, 577−582.
38. Sono, M., Andersson, L. A., and Dawson, J. H. (1982) *J. Biol. Chem. 257*, 8308−8320.
39. Berka, V., Palmer, G., Chen, P.-F., and Tsai, A.-L. (1998) *Biochemistry 37*, 6136−6144.

40. Hoffmann, K. (1953) in *Imidazole and Its Derivatives (Part I)*, pp 13−15, Interscience Publishers, New York.
41. Gorren, A. C. F., List, B. M., Schrammel, A., Pitters, E., Hemmens, B., Werner, E. R., Schmidt, K., and Mayer, B. (1996) *Biochemistry 35*, 16735−16745.
42. Ghosh, D. K., Wu, C., Pitters, E., Moloney, M., Werner, E. R., Mayer, B., and Stuehr, D. J. (1997) *Biochemistry 36*, 10609−10619.
43. Matsuoka, A., Stuehr, D. J., Olson, J., Clark, P., and Ikeda-Saito, M. (1994) *J. Biol. Chem. 269*, 20335−20339.
44. Frey, C., Narayanan, K., McMillan, K., Spack, L., Gross, S. S., Masters, B. S. S., and Griffith, O. W. (1994) *J. Biol. Chem. 269*, 26083−26091.
45. Salerno, J. C., McMillan, K., and Masters, B. S. S. (1996) *Biochemistry 35*, 11839−11845.
46. Schenkman, J. B., Remmer, H., and Estabrook, R. W. (1967) *Mol. Pharmacol. 3*, 113−123.
47. Kaufman, S. (1959) *J. Biol. Chem. 234*, 2677−2682.
48. Gachhui, R., Presta, A., Bentley, D. F., Abu-Soud, H. M., McArthur, R., Brudvig, G., Ghosh, D. K., and Stuehr, D. J. (1996) *J. Biol. Chem. 271*, 20594−20602.
49. Berka, V., Chen, P.-F., and Tsai, A.-L. (1996) *J. Biol. Chem. 271*, 33293−33300.
50. White, R. E., and Coon, M. J. (1982) *J. Biol. Chem. 257*, 3073−3083.
51. Abu-Soud, H. M., Loftus, M., and Stuehr, D. J. (1995) *Biochemistry 34*, 11167−11175.
52. Gorren, A. C. F., Schrammenl, A., Schmidt, K., and Mayer, B. (1997) *Biochemistry 36*, 4360−4366.
53. Presta, A., Siddhanta, U., Wu, C., Sennequier, N., Huang, L., Abu-Soud, H. M., Erzurum, S., and Stuehr, D. J. (1998) *Biochemistry 37*, 298−310.
54. Komori, Y., Hyun, J., Chiang, K., and Fukuto, J. M. (1995) *J. Biochem. 117*, 923−927.
55. Hofmann, H., and Schmidt, H. H. W. (1995) *Biochemistry 34*, 13443−13452.
56. Bublitz, C. (1977) *Biochem. Med. 17*, 13−19.
57. Chen, P.-F., Tsai, A.-L., and Wu, K. K. (1995) *Biochem. Biophys. Res. Commun. 215*, 1119−1129.
58. Martásek, P., Miller, R. T., Liu, Q., Roman, L. J., Salerno, J. C., Migita, C. T., Raman, C. S., Gross, S. S., Ikeda-Saito, M., and Masters, B. S. S. (1998) *J. Biol. Chem. 273*, 34799−34805.
59. Miller, R. T., Martásek, P., Raman, C. S., and Masters, B. S. S. (1999) *J. Biol. Chem. 274*, 14537−14540.
60. Ledbetter, A. P., McMillan, K., Roman, L. J., Masters, B. S. S., Dawson, J. H., and Sono, M. (1999) *Biochemistry 38*, 8014−8021.
61. Sono, M., McMillan, K., Roman, L. J., Masters, B. S. S., and Dawson, J. H. (1997) *J. Inorg. Biochem. 67*, 135 (Abstr.).

BI991580J